Journal of Materials Chemistry

Cite this: *J. Mater. Chem.*, 2011, **21**, 14663

www.rsc.org/materials

PAPER

Solution-processable π-conjugated dendrimers with hole-transporting, electroluminescent and fluorescent pattern properties

Zhong'an Li,[a] Zuoquan Jiang,[a] Shanghui Ye,[b] Cathy K. W. Jim,[c] Gui Yu,[b] Yunqi Liu,*[b] Jingui Qin,[a] Ben Zhong Tang[c] and Zhen Li*[a]

Received 19th March 2011, Accepted 22nd June 2011
DOI: 10.1039/c1jm11176k

In this paper, four new π-conjugated dendrimers **G1** and **G2-1**–**G2-3**, constructed by triphenylamine and carbazole moieties, have been successfully prepared *via* a simple synthetic route. This molecular design imparts the materials with good solution-processability, high thermal and morphological stabilities, and low oxidation potential, all of which are promising properties for optoelectronic materials. The double-layer OLEDs fabricated using these materials through solution processing demonstrate that they can exhibit dual functions, hole-transporting and light-emitting. Devices using **G1** or **G2-1** as the hole-transporting layer present good stability during the passage of current, with a maximum efficiency of 1.70 and 1.59 cd A^{-1}, respectively. Moreover, devices using these dendrimers as the emitting layer show moderate performance, and the device of **G2-2** gives a maximum luminance and efficiency of 1190 cd m^{-2} and 1.67 cd A^{-1}, respectively, thanks to three-dimensional building of the dendritic system, which might suppress the inherent reductive or aggregation-caused quenching that usually happens for triphenylamine/carbazole derivatives to some degree. Also, the photo-cross-linking property of triple bonds enables ready fabrication of highly fluorescent photoresist patterns of these dendrimers.

Introduction

Since the milestone discovery of Kodak's team[1] and Cambridge's group,[2] organic light-emitting diodes (OLEDs) have been the subject of wide investigations from both academic and industrial laboratories. Nowadays, OLEDs have been seriously considered as the next generation full-color flat-panel displays, owing to their superior properties to existing flat-panel displays like liquid crystal displays (LCDs) and plasma display panels (PDPs), such as being relatively thin, light, possessing excellent color purity and power efficiency.[3–7] According to the aimed applications, great efforts have been taken to optimize the device architectures, as well as to develop new materials including both charge transporting materials and light emitters. Following the conventional conjugated small molecules and polymers, π-conjugated dendrimers are now regarded as the third class of materials for use in OLEDs, thanks to their unusual molecular structures, electrical and optical properties. Generally, dendrimers are usually composed of a core, dendrons, and surface groups, and by careful structural design, they can combine the merits of well-defined structures, the superior chemical purity possessed by small molecules and the simple solution-processing advantage of polymers, making them a very promising alternative for OLED fabrications.[8] Furthermore, another key feature of π-conjugated dendrimers attracting great interest of researchers is that such large dendritic topology can provide a facile way to tune the emission through the modulation of their electronic properties, and control intermolecular interactions at the molecular level.[9] In recent years, great progress has been made in both the development of novel optoelectronic dendrimers and highly efficient dendrimer devices.[8–12] Consequently, it is critical to develop new materials and devices to make these applications more feasible, and for chemists, considerable work should be carried out to reveal how the chemical composition, geometric structure, and packing influence the final device properties when developing new materials.

During the past few decades, triphenylamine and carbazole derivatives have been widely investigated due to their excellent charge transporting properties and reasonably high thermal stabilities as hole-transporting materials for optoelectronic applications.[13–18] For example, certain triphenylamines derivatives such as TPD (*N*,*N*-diphenyl-*N*,*N*-bis(*m*-toly)benzidine) and NPB (*N*,*N*-dinaphthyl-*N*,*N*-diphenylbenzidine), as well as carbazole-containing polymers or small molecules, such as PVK (polyvinylcarbazole) and CBP (*N*,*N*-dicarbazolyl-4,4-biphenyl) are widely used as hole-transporting materials in multilayer

[a]*Department of Chemistry, Hubei Key Lab on Organic and Polymeric Opto-Electronic Materials, Wuhan University, Wuhan, 430072, China. E-mail: lizhen@whu.edu.cn; lichemlab@163.com; Fax: +86-27-68756757; Tel: +86-27-62254108*
[b]*Organic Solids Laboratories, Institute of Chemistry, The Chinese Academy of Sciences, Beijing, 100080, China. E-mail: liuyq@iccas.ac.cn.*
[c]*Department of Chemistry, The Hong Kong University of Science & Technology, Clear Water Bay, Kowloon, Hong Kong, China*

OLEDs.[15,19–21] Additionally, they were recently reported to effectively act as hosting materials in highly efficient blue, green, or red electrophosphorescence devices, due to their high triplet energy.[22–26] However, most triarylamines or carbazole derivatives are usually either non-luminescent or only weakly emitting, as a result of the inherent reductive quenching and possible exciplex formation.[27,28] As is well known, the composition of OLEDs can largely be divided into hole-transport, electron-transport, emission layer and electrode types according to their characteristics. Through the proper choice of electron-, hole-transport and emission materials, a better efficiency could be achieved in the multilayer device.[29] Thus, if a layer could possess dual functions, light emitting and hole transporting, it would be a good alternative to reduce the production costs for the resultant applications, *i.e.*, Lin and co-workers have found a series of arylamines end-capped with 3,6-carbazole to be potential green- or blue-emitters and capable of hole transporting.[30]

With all the above thoughts in mind, and to develop the family of materials with dual functions for OLEDs applications, in this paper, we described the preparation of a new series of π-conjugated dendrimers of the first and second generations (**G1** and **G2-1**–**G2-3**) incorporating triphenylamine and carbazole moieties (Scheme 1–3). The thermal stability, optical, electrochemical behaviours of these dendrimers were systematically studied, and in an effort to utilize these dendrimers in OLEDs, we have fabricated two types of double-layer devices to investigate their hole-transporting and electroluminescent properties.

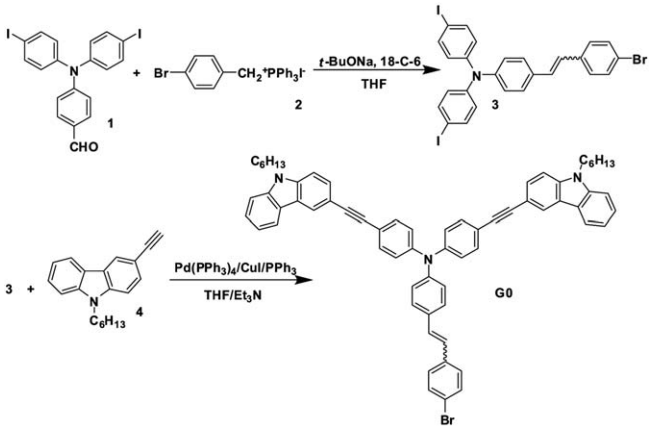

Scheme 1 Synthetic route of **G0**.

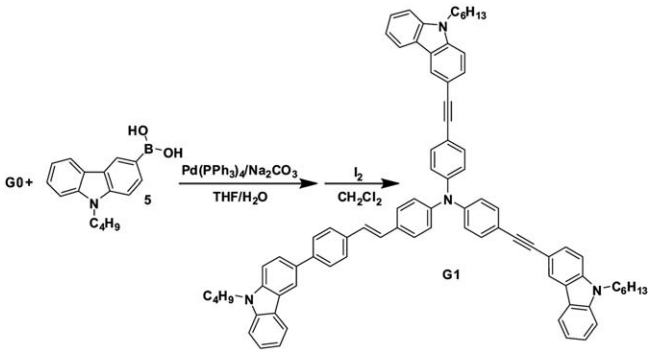

Scheme 2 Synthetic route of **G1**.

Results and discussion

Synthesis and characterization

Herein, as shown in Scheme 1–3, the efficiency of the synthetic approach to the first and second π-conjugated dendrimers (**G1** and **G2-1**–**G2-3**) is moderate, with no need to protect/de-protect some functional groups or include the converting process from one reactive group to another, by taking advantage of their easy handling at the three active 4-positions of the triphenylamine moieties and the 3-, 6-, or 9-positions of the carbazole moieties. First, Vilsmeier reaction of the triphenylamine molecule and subsequent Tuker iodination afforded 4-(bis(4-iodophenyl) amino)benzaldehyde (**1**), which further reacted with (4-bromobenzyl)triphenylphosphonium bromide (**2**) to give an *E*- and *Z*-isomer mixture of compound **3** in moderate yield (61.8%). As we know, aryl, bromide, and iodine moieties exhibit different reaction activities to process the Sonogashira coupling reaction, so here, by controlling room temperature, and being catalyzed by $Pd(PPh_3)_4$, PPh_3 and CuI, 3-ethynyl-9-hexylcarbazole (**4**) was used to react with the aryl-iodine groups of compound **3** to produce important intermediate **G0** with a good yield (79.4%). Finally, a typical Suzuki reaction between **G0** and 3-boronic acid-9-butyl-carbazole (**5**) or borates **6–8** gave the desired dendrimers **G1** and **G2** as a mixture of *E*- and *Z*-isomers, and then the pure *E*-isomer could be obtained by refluxing using a small catalytic amount of I_2. The yield of these two steps is satisfying (70.9–90.0%), considering the rigidity and steric hindrance within the large molecule of **G0**.

All of the resultant dendrimers are quite stable toward air and are readily soluble in common organic solvents such as $CHCl_3$, CH_2Cl_2 and THF, while their thin films can be easily obtained by spin-coating the materials onto glass slides. We carefully confirmed the structures of the dendrimers **G1** and **G2** by ^1H and ^{13}C NMR spectroscopy, mass spectrometry, and elemental analysis. The observed peaks in the ^1H NMR spectra are readily assigned to the resonances of the appropriate protons as demonstrated in Scheme 1–3, and no unexpected peaks appear. Fig. 1 gives the ^1H NMR spectra of **G0** and **G2-2** for example. After the reaction between **G0** and borate **7**, the proton peaks derived from *Z*–C═CH of **G0** disappear, while those associated with the 9-NCH_2, 5-ArH, and 4-ArH protons of the carbazole rings at around 4.3, 8.1 and 8.3 ppm, respectively, can be still observed in the spectrum of **G2-2**. In addition, it is easily seen that a new triple peak associated with the -OCH_2- of compound **7** appears in the ^1H NMR spectrum of **G2-2**, indicating the success of the preparation of **G2-2**. On the other hand, the signal assigned to the molecular ions in MALDI-TOF MS can directly verify the presence of the desired dendrimers **G1** and **G2**, and the detailed data are summarized in Table 1.

Thermal analysis

The thermal stabilities of the dendrimers were examined by thermogravimetric analysis (TGA) and differential scanning calorimetry (DSC) in N_2 at a heating rate of 10 °C min^{-1}, with the results listed in Table 1. As shown in Fig. 2, all of dendrimers are thermally stable, with decomposition temperatures (T_d, corresponding to a 5% weight loss) in the range of 290–374 °C. It is

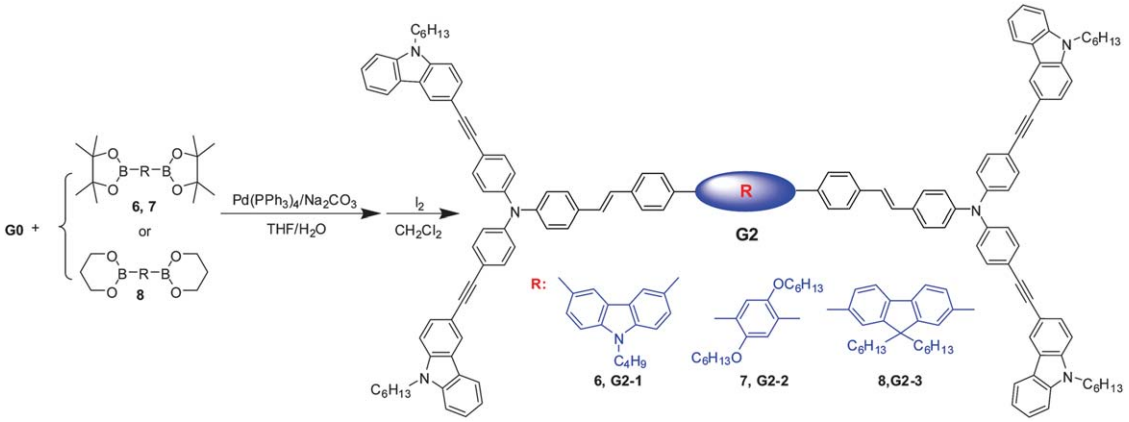

Scheme 3 Synthetic route of **G2**.

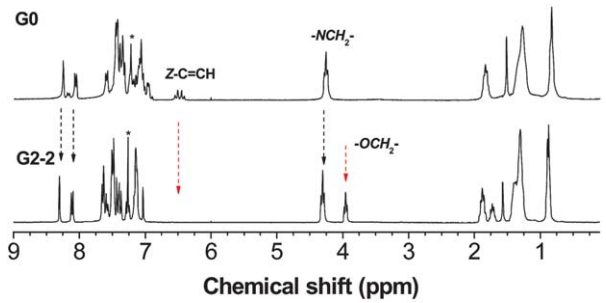

Fig. 1 The ^{1}H NMR spectra of dendrimers **G0** and **G2-2**, conducted in chloroform-*d* (*).

Table 1 Characterization results of dendrimers

No.	Yield (%)	*m*/*z*[a]	*m*/*z* (calc.)[b]	T_d/°C[c]
G1	70.9	1114.6	1114.4	339
G2-1	71.1	2007.1	2006.5	374
G2-2	73.3	2062.1	2061.7	373
G2-3	90.0	2118.2	2118.4	290

[a] Measured by MALDI-TOF mass spectrometry. [b] Calculated for [M + H]$^+$. [c] The 5% weight loss temperature of polymers detected by the TGA analyses under nitrogen at a heating rate of 10 °C min^{-1}.

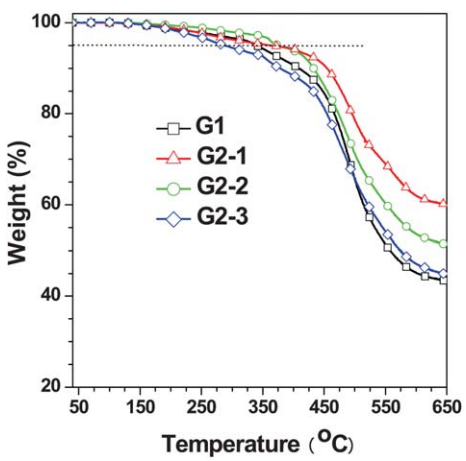

Fig. 2 TGA curves of dendrimers **G1** and **G2**.

a pity that the glass transition temperatures (T_g) of these dendrimers could not be determined clearly.

Optical properties

In order to investigate the photophysical properties of the dendrimers, their UV-vis absorption and photoluminescent (PL) spectra in dilute THF solutions and in solid films were investigated, with the characteristic data listed in Table 2. For the UV-vis absorption spectra in THF solutions (Fig. 3a), the first generation dendrimer (**G1**) exhibits two absorption peaks at around 293 and 383 nm, which are ascribed to the absorption of the carbazole moieties and π–π* transition, respectively. All the second generation dendrimers (**G2-1**–**G2-3**) display very similar absorption bands as **G1** with the same absorption maxima, meaning that **G1** and **G2** contain the same effective conjugation length in the ground state. This observation indicates that the dendrimer generation does not play a key role in the photophysical properties within such giant architectures.[31–33] Moreover, the intensity of the peak at about 293 nm for **G2** decreases in comparison with that of **G1**, possibly because the relative number of carbazole moieties compared to the number of π–π* transition in **G2**[34] is reduced. Fig. 3b gives UV-vis spectra of dendrimers in the solid state, and their behaviours are quite similar to those in dilute solutions. Nevertheless, the absorption bands of both **G1** and **G2** become a little broad, as well as the slight red shift (9–12 nm) to longer wavelength being attributed to aggregation effects. In addition, unlike the other two **G2** dendrimers, **G2-3** shows a distinctively different absorption

Table 2 Optical properties of polymers in solution and the solid state

No.	$\lambda_{Abs,\ sol}$[a]/nm	$\lambda_{PL,sol}$[a]/nm	$\lambda_{Abs,\ film}$[b]/nm	$\lambda_{PL,film}$[b]/nm	Φ_F[c]
G1	383	456	395	460	0.64
G2-1	384	455	393	462	0.76
G2-2	383	460	392	465	0.80
G2-3	383	469	395	469	0.80

[a] The maximum absorption and emission wavelength of dendrimer solutions in THF solutions, where the concentration is 5 × 10^{-6} mol L^{-1}. [b] The maximum absorption and emission wavelength of dendrimer in the solid state. [c] Quantum yields in THF solutions using 9,10-diphenylanthracene in cyclohexane (Φ_F = 90%) as standard.

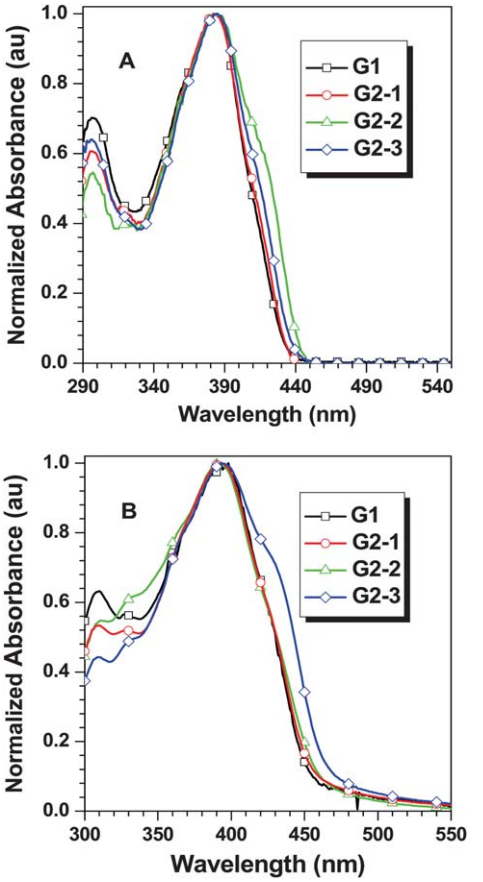

Fig. 3 The UV-vis spectra of dendrimers in THF solutions (A) and in films (B).

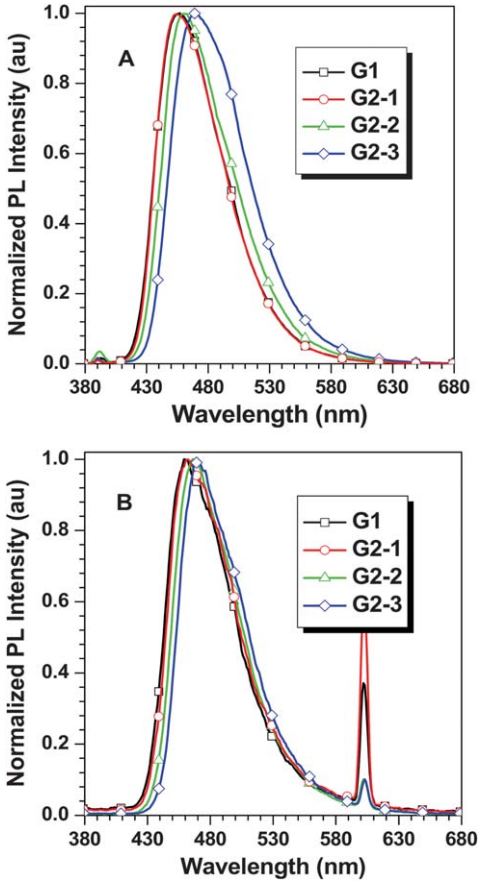

Fig. 4 The PL spectra of dendrimers in THF solutions (A) and in films (B). Excitation wavelengths (nm): 390 for **G1**, 395 for **G2-1**, 389 for **G2-2**, and 392 for **G2-3**.

spectrum as a thin film with a pronounced shoulder peak in comparison with its corresponding absorption in solution, generally indicating a strong intermolecular packing in the solid state caused by the more planar and rigid backbones while using fluorene as the core.

The PL spectra of the dendrimers in dilute THF solutions and in the solid state are displayed in Fig. 4 and all the dendrimers exhibited similar PL behaviours: an emission peak at 455–469 nm with a narrow full width at half-emission maximum (fwhm) of 55–62 nm. In solution, the emission peak of dendrimer **G1** locates at 456 nm, while that of **G2-1** is at 455 nm, with almost no change with a larger conjugation system. By contrast, the emission maxima for **G2-2** and **G2-3** are red shifted by 4 and 13 nm, respectively, compared to that of **G1**. It is reasonable that for the structure of **G2-1**, the peripheral dendrons do not efficiently conjugate to the core because of the usage of the non-planar 3,6-carbazole linkage; however, the planarity can be enhanced gradually from the 1,4-benzene to the 2,7-fluorene linkage as the core, thus resulting in much more efficient intramolecular charge transport between dendrons. Furthermore, we also investigated the PL quantum yields (Φ_F, Table 2) of the dendrimers using 9,10-diphenylanthracene in cyclohexane (Φ_F = 90%) as reference, and the Φ_F value of **G1** was measured to be 0.64, while those of **G2** are a little higher, 0.76–0.80, due to more efficient energy transport. The PL spectra of dendrimers in the solid state are shown in Fig. 4b, and the emission peaks locate at 460–469 nm, all of which are red-shifted in comparison with those in solutions. Generally, using the acetylene linkages to construct conjugated molecules containing dendrimers always allows them to adopt a more planar structure, inducing serious π–π stacking

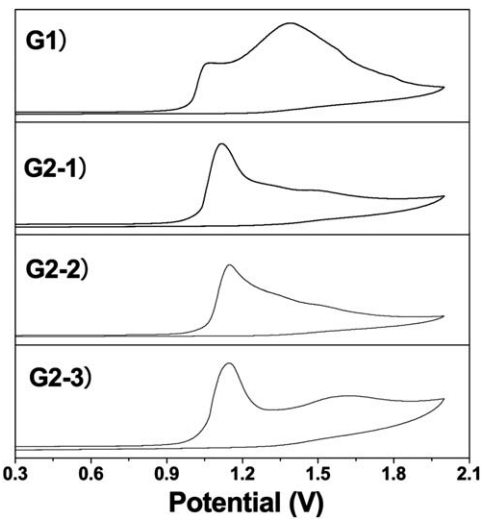

Fig. 5 Cyclic voltammograms of the dendrimer films on Pt working electrode *versus* Fc/Fc^+.

Table 3 Electrochemical properties of dendrimers

No.	E_g^{opt}/eV[a]	$E_{onset,(ox)}$/V *vs.* FOC[b]	E_{HOMO}/eV[c]	E_{LUMO}/eV[d]
G1	2.75	0.50	−5.30	−2.55
G2-1	2.71	0.54	−5.34	−2.63
G2-2	2.70	0.55	−5.35	−2.65
G2-3	2.68	0.53	−5.33	−2.65

[a] Band gaps obtained from absorption edge in film ($E_g^{opt} = 1240/\lambda_{onset}$). [b] The first onset oxidation potential *vs.* Fc/Fc$^+$ ($E_{onset(ox),FOC}$). [c] $E_{HOMO} = -(E_{onset(ox),FOC} + 4.8)$ eV. [d] $E_{LUMO} = E_{HOMO} + E_g$.

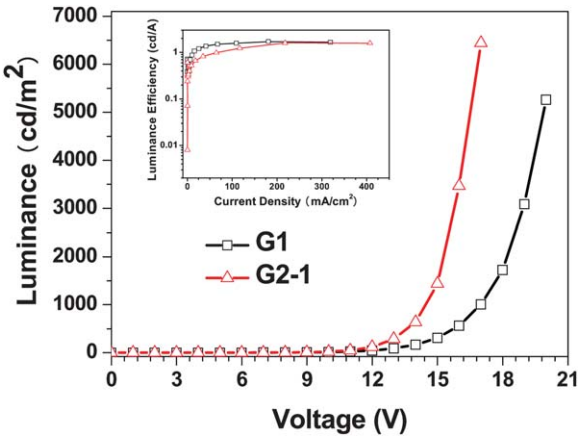

Fig. 6 Luminance–voltage characteristics of the OLEDs using dendrimers as a hole-transporting layer; inset: the luminescence efficiency–current characteristics of the OLEDs.

in the solid state, and thus luminescence will be quenched accompanied by a red-shift in emission.[9,35] As shown in Table 2, the red shifted degree of **G1** and **G2** is not serious to any extent, and the peak shape only changes a little (fwhm values are still around 60 nm), in relation to the phenomena observed in linear molecules. These results indicate the absence of aggregation in the dendrimers to some degree because of their three-dimensional dendritic structure, and the usage of non-coplanar triphenylamines.

Electrochemistry properties

The electrochemical properties of the films of the dendrimers coated on a Pt working electrode were investigated by cyclic voltammetry carried out in tetrabutylammonium perchlorate–CH_3CN solution at a scan rate of 100 mV s^{-1}. The cyclic voltammograms (CVs) are shown in Fig. 5, and the relative data of the energy levels are summarized in Table 3. It is obvious that all the dendrimers display irreversible oxidation peaks, and their onset oxidation potentials ($E_{onset(ox)}$) were measured to be 0.50–0.55 *vs.* Fc/Fc$^+$. The highest-occupied molecular orbital (HOMO) energy levels of the dendrimers were obtained based on $E_{onset(ox)}$ with reference to ferrocene (4.8 eV), according to the following equation: $E_{HOMO} = -(E_{onset(ox),FOC} + 4.8)$ eV, and ranged from −5.30 to −5.35 eV. Then, their LUMO (lowest unoccupied molecular orbital) levels were calculated to be between −2.55 and −2.65 eV, by subtracting the energy band gaps (E_g^{opt}, 2.68–2.75 eV) from the HOMO energy level. As a result, the high-lying HOMO energy levels and irreversible electrochemical oxidations of the dendrimers suggest that these compounds have potential abilities for hole injection and transport, while the low-lying energy levels mean that they can capture electrons released from the cathode and may lead to improved performance.

Table 4 EL data of OLEDs using dendrimers as a hole-transporting layer

No.	V_{on}[a]/V	Lumin.[b] L/cd m^{-2}	CD[c] J/mA cm^{-2}	CE[d]/cd A^{-1}
G1	4.0	5262	319	1.70
G2-1	4.0	6443	407	1.59

[a] Turn-on voltage. [b] Maximum luminance. [c] Current density at the maximum luminance. [d] Maximum luminescence efficiency.

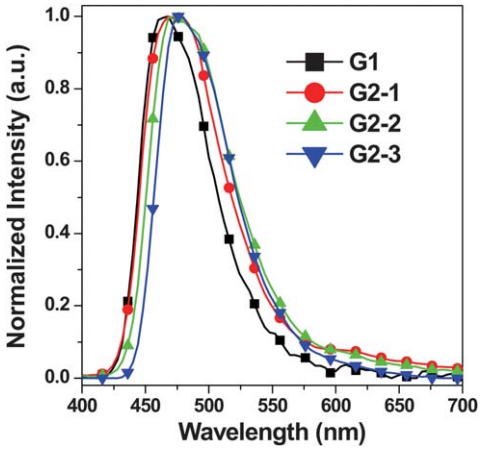

Fig. 7 The EL spectra of OLEDs using dendrimers as emitting layer.

Electroluminescent properties

First, the hole-transport abilities of dendrimers **G1** and **G2-1** were investigated in double-layer OLEDs with a configuration of ITO/**G1** or **G2-1**(80 nm)/Alq3(60 nm)/Ca:Ag(100 nm), in which **G1** or **G2-1** was used as a hole-injecting and -transporting layer through spin-coating processing and Alq3 was used as an emitting layer as well as an electron-transporting layer. When a bias potential was applied to the electrodes, both devices showed identical electroluminescence (EL) peaks at about 530 nm, originating from Alq3, indicating that both **G1** and **G2-1** only serve as hole-transporting materials without causing exciplex formation at the interface with Alq3. The luminance–voltage and luminescence efficiency–current density characteristics of these two devices are shown in Fig. 6, and the results are summarized in Table 4. Both devices demonstrate the same and low turn-on voltage of 4 V due to their proper HOMO energy level, and the device of **G2-1** shows a slightly better maximum brightness of 6443 cd m^{-2} at 17 V than that of the **G1**-based device (5262 cd m^{-2} at 20 V); however, the maximum luminescence efficiency of the latter (1.70 cd A^{-1}) is a little higher in comparison with that of former (1.59 cd A^{-1}). It is noticeable that both devices present good stability during the passage of current, and can nearly

Table 5 EL data of OLEDs using dendrimers as an emitting layer

No.	$\lambda_{EL,max}$[a]/ nm	V_{on}[b]/ V	Lumin.[c] L/cd m^{-2}	CD[d] J/mA cm^{-2}	CE[e]/ cd A^{-1}	CIE[f]
G1	468	3.0	185	139	0.31	0.148, 0.247
G2-1	468	3.0	563	304	0.72	0.173, 0.248
G2-2	472	3.0	1190	299	1.67	0.173, 0.294
G2-3	476	3.5	847	320	0.89	0.157, 0.324

[a] The EL wavelengths. [b] Turn-on voltage. [c] Maximum luminance. [d] Current density at the maximum luminance. [e] Maximum luminescence efficiency. [f] Commission International de L'Eclairage coordinates (x, y).

retain their maximum luminance efficiency with little change even at the current density of ~400 mA cm^{-2}. The good performances obtained from these devices demonstrate that these dendrimers could be a promising candidate for hole-transporting materials, which are attributed to their relatively high-lying HOMO energy levels, along with good morphological and thermal stabilities.

Secondly, we also fabricated another type of double-layer OLED (ITO/**G1** or **G2**(50 nm)/TPBI(30 nm)/LiF(1 nm)/Al (100 nm)) to study the light-emitting properties of these dendrimers, in which dendrimers **G1** and **G2** had dual functionalities (emitting layer and hole injection/transport layer) because of their good hole-transporting abilities as demonstrated above, and TPBI was adopted as an electron-transporting layer and hole-blocking layer. With a low turn on voltage (3.0–3.5 V), bright green-blue EL emissions at around 470 nm can be achieved from their EL devices (Fig. 7), and the Commission Internationale d'Eclairage (CIE) data are listed in Table 5. In addition, the EL spectra are very narrow, with fwhm values of 60 nm, which corresponded well with their PL curves, indicating that the intermolecular interactions between the molecules are very weak, thanks to the three-dimensional dendritic structure.

Fig. 8 gives the voltage–luminance and voltage–current density characteristics of these devices, and all demonstrate reliable EL performances. As shown in Table 5, the maximum current density and luminance of the **G1**-based device is 139 mA cm^{-2} and 185 cd m^{-2} at 13 V, respectively, whereas those of the other

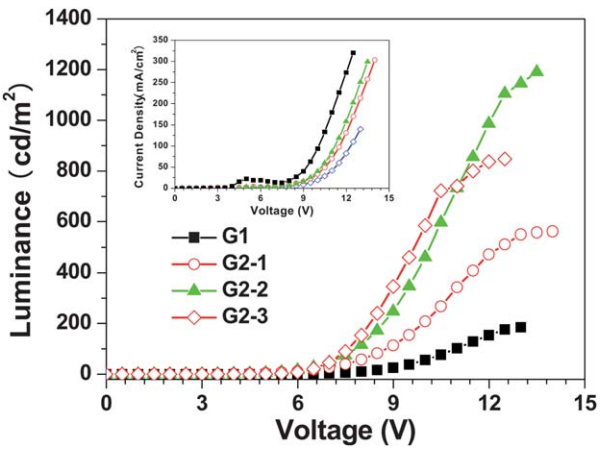

Fig. 8 Luminance–voltage characteristics of the OLEDs using dendrimers as the emitting layer; inset: current–voltage characteristics of the OLEDs.

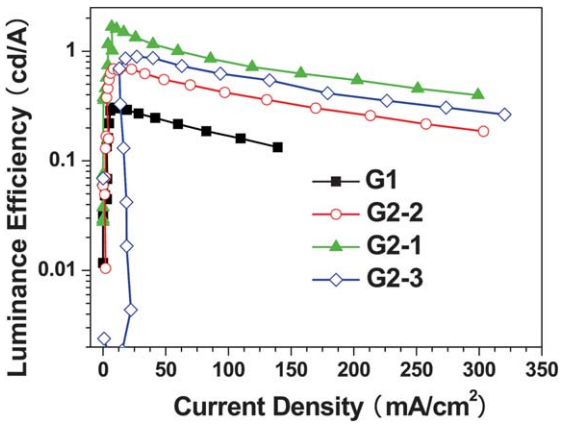

Fig. 9 The luminescence efficiency–current characteristics of OLEDs using dendrimers as the emitting layer.

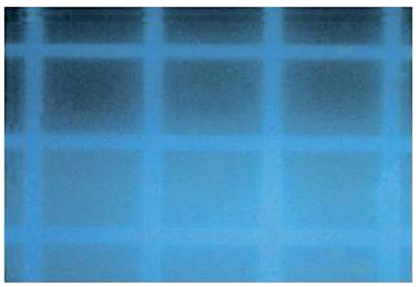

Fig. 10 Photoresist pattern of **G2-1** taken under UV lamp illumination.

three second generation dendrimer (**G2**)-based devices can improve much better at a similar voltage, and in particular, **G2-2** exhibits a maximum current density and luminance of 299 mA cm^{-2} and 1190 cd m^{-2} at 13.5 V, respectively, although this device is non-optimized. The luminescence efficiency–current characteristics of the devices (Fig. 9) indicate that **G2-2** also possesses the highest maximum luminescence efficiency compared to other dendrimers, up to 1.67 cd A^{-1}, suggesting that the inherent reductive or aggregation-caused quenching might be suppressed to some degree.

The luminescent imaging soft photolithography technique has potential applications in photonic and electronic devices and biological sensing and probing chips.[36] Also, it is well known that acetylenic triple bonds are readily photo-cross-linkable,[37] thus, as an example, exposure of dendrimer **G2-1** to UV light followed by development results in the formation of a negative photoresist pattern. As shown in Fig. 10, the pattern with regularly arranged grids can emit blue light under a fluorescence microscope.

Conclusions

In summary, a series of new solution-processable π-conjugated dendrimers based on triphenylamine/carbazole moieties have successfully been developed through a simple route, and exhibit comprehensive properties, such as good solution-processability, thermal and morphological stabilities, and low oxidation potential. Double-layer Alq3 emitting OLEDs using **G1** and **G2-1** as hole-transporting materials were fabricated, and the devices

show good performance and satisfactory efficiency stability during the passage of current. Meanwhile, the usage of dendrimers as emissive materials for OLEDs was also investigated, where the device based on **G2-2** exhibits a better performance with a maximum luminance and efficiency of 1190 cd m^{-2} and 1.67 cd A^{-1}, respectively. Therefore, the results of this paper demonstrate that these dendritic materials, for second generation dendrimers (**G2**) in particular, exhibit both light-emitting and hole-transporting abilities through rational structure design, which is promising for OLEDs applications. In addition, the photo-cross-linking experiments suggest that the triple bonds in these dendrimers can allow their films to be patterned into fluorescent images.

Experimental section

Materials

Tetrahydrofuran (THF) was dried over and distilled from a K–Na alloy under an atmosphere of dry nitrogen. Triethylamine (Et_3N) was distilled under normal pressure and kept over potassium hydroxide. Compounds **1–2** and **4–7** were prepared as in our previous work or according to the literature method.[38–43] All other reagents were used as received.

Instrumentation

The ^1H and ^{13}C NMR spectra were measured on a Varian Mercury300 spectrometer using tetramethylsilane (TMS; δ = 0 ppm) as internal standard. Matrix-assisted laser desorption ionization time-of-flight mass spectra were measured on a Voyager-DE-STR MALDI-TOF mass spectrometer (MALDI-TOF MS; ABI, American) equipped with a 337 nm nitrogen laser and a 1.2 m linear flight path in positive ion mode. Elemental analyses were performed by a CARLOERBA-1106 micro-elemental analyzer. UV-visible spectra were obtained using a Shimadzu UV-2550 spectrometer. PL spectra were recorded on Hitachi F-4500 fluorescence spectrophotometer. Thermal analysis was performed on NETZSCH STA449C thermal analyzer at a heating rate of 10 °C min^{-1} in nitrogen at a flow rate of 50 cm^3 min^{-1} for thermogravimetric analysis (TGA). The thermal transitions were investigated using a METTLER differential scanning calorimeter DSC822e under nitrogen at a scanning rate of 10 °C min^{-1}. Cyclic voltammetry (CV) was carried out on a CHI voltammetric analyzer in a three-electrode cell with a Pt counter electrode, a Ag/AgCl reference electrode, and a glassy carbon working electrode at a scan rate of 100 mV s^{-1} with 0.1 M tetrabutylammonium perchlorate (purchased from Alfa Aesar) as the supporting electrolyte, in anhydrous acetonitrile solution purged with nitrogen. The potential values obtained in reference to the Ag/Ag^+ electrode were converted to values *versus* the saturated calomel electrode (SCE) by means of an internal ferrocenium/ferrocene (Fc^+/Fc) standard.

Synthesis of compound 3

To a solution of compound **1** (2.85 g, 5.37 mmol) and compound **2** (2.92 g, 6.96 mmol) in dry THF (22 mL), was added potassium *tert*-butoxide (1.82 g, 16.25 mmol) and a catalytic amount of 18-C-6 under argon. The mixture was stirred in the absence of light at room temperature overnight, and then a lot of water was added into the reaction solution. The resultant mixture was extracted with $CHCl_3$, washed with brine, dried over anhydrous Na_2SO_4, and evaporated to dryness. The crude product was purified by column chromatography on silica gel using chloroform/petroleum ether (1 : 2, v/v) as eluent to afford yellow solid **3** (2.25 g, 61.8%). ^1H NMR (300 M Hz, $CDCl_3$, 298 K, *E*-isomer) δ (ppm): 6.82 (m, 4H, ArH), 6.89 (m, 2H, –C═CH), 7.0–7.16 (m, 2H, ArH), 7.35 (m, 4H, ArH), 7.53 (m, 6H, ArH).

Synthesis of dendrimer G0

A mixture of compound **3** (1.93 g, 2.85 mmol), compound **4** (1.71 g, 6.19 mmol), cuprous iodide (CuI) (70 mg, 0.37 mmol), triphenylphosphine (PPh_3) (100 mg, 0.38 mmol), tetrakis(triphenylphosphine)palladium ($Pd(PPh_3)_4$) (70 mg, 0.06 mmol), and THF (22 mL)/Et_3N (27 mL) was carefully degassed and charged with nitrogen. The reaction was stirred for 3 days at room temperature. The mixture was extracted with $CHCl_3$, washed with water, dried over anhydrous Na_2SO_4, and evaporated to dryness. The crude product was purified by column chromatography on silica gel using chloroform/petroleum ether (1 : 2, v/v) as eluent to afford yellow solid **G0** (2.20 g, 79.4%). ^1H NMR (300 M Hz, $CDCl_3$, 298 K, *E*-isomer) δ (ppm): 0.86 (m, 6H, $–CH_3$), 1.31 (m, 12H, $–CH_2–$), 1.88 (m, 4H, $–CH_2–$), 4.30 (t, J = 7.5 Hz, 4H, $–NCH_2–$), 6.99 (q, J = 16.2 Hz, 2H, –C═CH), 7.13 (m, 6H, ArH), 7.23 (m, 2H, ArH), 7.28–7.49 (m, 16H, ArH), 7.51 (d, J = 8.7 Hz, 2H, ArH), 8.09 (d, J = 7.5 Hz, 2H, ArH), 8.29 (s, 2H, ArH). $C_{66}H_{58}BrN_3$ (EA) (%, found/calcd): C, 81.88/81.46; H, 6.06/6.01; N, 3.98/4.32.

Synthesis of dendrimer G1

A mixture of **G0** (117 mg, 0.12 mmol), the boronic acid **5** (35 mg, 0.13 mmol), sodium carbonate (130 mg, 1.22 mmol), THF (6 mL)/water (2 mL), and tetrakis(triphenylphosphine)palladium ($Pd(PPh_3)_4$) (7 mg) was carefully degassed and charged with nitrogen. The reaction was stirred at 80 °C for about 30 h. After being cooled to room temperature, the organic layer was extracted with $CHCl_3$, dried over anhydrous Na_2SO_4, and evaporated to dryness. The crude product was purified by column chromatography on silica gel using chloroform/petroleum ether (1 : 1) to afford the compound containing *E*- and *Z*-isomers. Then, the above resultant product with a catalytic amount of I_2 was dissolved in CH_2Cl_2, and then charged with nitrogen. The mixture was stirred at 60 °C for about 6 h without light. After the reaction was cooled, the aqueous solution of NaS_2O_3 was added and stirred for 0.5 h. The organic layer was separated, dried over anhydrous Na_2SO_4, and evaporated to dryness. The crude product was purified by column chromatography to afford the pure *E*-isomer **G1** (95 mg, 70.9%). ^1H NMR (300 MHz, $CDCl_3$, 298 K) δ (ppm): 0.85 (br, s, 6H, $–CH_3$), 0.96 (t, J = 7.5 Hz, 3H, $–CH_3$), 1.24–1.40 (m, 16H, $–CH_2–$), 1.86 (m, 6H, $vCH_2–$), 4.31 (m, 6H, $–NCH_2–$), 7.13 (d, J = 8.7 Hz, 8H, ArH and C═CH), 7.23 (m, 3H, ArH), 7.34–7.50 (m, 16H, ArH), 7.60 (m, 3H, ArH), 7.62 (m, 3H, ArH), 8.07 (d, J = 8.1 Hz, 2H, ArH), 8.13 (d, J = 7.2 Hz, 1H, ArH), 8.28 (s, 2H, ArH), 8.33 (s, 1H, ArH). ^{13}C NMR (75 MHz, $CDCl_3$, 298 K) δ (ppm): 13.91, 14.00, 20.60, 22.55, 26.96, 28.95, 29.73, 31.19, 31.57, 42.98, 43.23,

87.55, 90.60, 108.73, 108.92, 113.45, 118.21, 118.63, 118.94, 119.30, 120.46, 120.55, 122.52, 122.90, 123.00, 123.41, 123.78, 123.92, 124.94, 125.82, 126.06, 126.89, 127.42, 127.53, 129.24, 131.75, 132.58, 133.01, 135.65, 140.06, 140.84, 140.95, 141.22, 146.23, 146.67. MALDI-TOF-MS: calcd for ($C_{82}H_{74}N_4$): *m/z* [M^+]: 1114.6; found: *m/z* 1114.4. $C_{84}H_{78}N_4$ (EA) (%, found/calcd): C, 87.93/88.29; H, 7.19/6.69; N, 5.02/5.02.

General procedure of the synthesis of dendrimers G2

A mixture of compound **G0** (~2.10 equiv), the borate **6–8** (1.0 equiv.), sodium carbonate (10.0 equiv.), THF (the concentration of borate is about 0.005 M)/water (3 : 1 in volume), and tetrakis (triphenylphosphine)palladium ($Pd(PPh_3)_4$) (3–5 mol %) was carefully degassed and charged with nitrogen. The reaction was stirred at 80 °C for about 30 h. After it was cooled to room temperature, the organic layer was extracted with $CHCl_3$, dried over anhydrous Na_2SO_4, and evaporated to dryness. The crude product was purified by column chromatography to afford the compound containing *E*- and *Z*-isomers. Then, the above resultant product with a catalytic amount of I_2 was dissolved in CH_2Cl_2, and charged with nitrogen. The mixture was stirred at 60 °C for about 6 h without light. After the reaction was cooled, the aqueous solution of $Na_2S_2O_3$ was added and stirred for 0.5 h. The organic layer was separated, dried over anhydrous Na_2SO_4, and evaporated to dryness. The crude product was purified by column chromatography to afford the pure *E*-isomer.

G2-1. Compound **G0** (215 mg, 0.22 mmol), borate **6** (50 mg, 0.11 mmol). The crude product was purified by column chromatography on silica gel using chloroform/petroleum ether (3 : 2, v/v) as eluent to afford a yellow solid (150 mg, 71.1%). ^{1}H NMR (300 MHz, $CDCl_3$, 298 K) δ (ppm): 0.89 (m, 15H, $-CH_3$), 1.2–1.5 (m, 28H, $-CH_2-$), 1.87 (m, 10H, $-CH_2-$), 4.31 (t, $J = 7.2$ Hz, 10H, $-NCH_2-$), 7.14 (m, 16H, ArH and C=CH), 7.23 (m, 4H, ArH), 7.36–7.51 (m, 24H, ArH), 7.63 (d, $J = 9.0$ Hz, 8H, ArH), 7.77 (m, 6H, ArH), 8.09 (d, $J = 7.2$ Hz, 4H, ArH), 8.30 (s, 4H, ArH), 8.41 (s, 2H, ArH). ^{13}C NMR (75 MHz, $CDCl_3$, 298 K) δ (ppm): 14.22, 22.77, 27.20, 29.18, 29.94, 31.80, 43.47, 87.74, 90.77, 108.96, 109.14, 113.65, 148.42, 119.51, 120.78, 122.73, 123.11, 124.00, 124.14, 125.13, 126.28, 127.15, 127.79, 129.45, 132.80, 136.0, 140.26, 141.05, 146.50, 146.78. MALDI-TOF-MS: calcd for ($C_{148}H_{131}N_7$): *m/z* [M^+]: 2007.1; found: *m/z* 2006.5. $C_{84}H_{72}N_4$ (EA) (%, found/calcd): C, 88.75/88.54; H, 6.94/6.58; N, 4.68/4.88.

G2-2. Compound **G0** (215 mg, 0.22 mmol), borate **7** (56 mg, 0.11 mmol). The crude product was purified by column chromatography on silica gel using chloroform/petroleum ether (3 : 2, v/v) as eluent to afford a yellow solid (160 mg, 73.3%). ^{1}H NMR (300 MHz, $CDCl_3$, 298 K) δ (ppm): 0.87 (m, 18H, $-CH_3$), 1.2–1.5 (m, 36H, $-CH_2-$), 1.73 (m, 4H, $-CH_2-$), 1.88 (m, 8H, $-CH_2-$), 3.94 (t, $J = 6.6$ Hz, 4H, $-OCH_2-$), 4.31 (t, $J = 7.2$ Hz, 8H, $-NCH_2-$), 7.04 (s, 2H, ArH), 7.15 (m, 16H, ArH and C=CH), 7.26 (m, 4H, ArH), 7.37–7.67 (m, 36H, ArH), 8.10 (d, $J = 7.2$ Hz, 4H, ArH), 8.30 (s, 4H, ArH). ^{13}C NMR (75 MHz, $CDCl_3$, 298 K) δ (ppm): 14.29, 22.80, 22.86, 26.03, 27.20, 29.19, 29.56, 31.72, 31.81, 43.45, 69.82, 87.72, 90.77, 108.96,109.15, 113.55, 116.21, 118.35, 119.50, 120.77, 122.67, 123.06, 123.99, 124.14, 125.09, 126.28, 127.81, 127.99, 129.43, 130.06, 130.56, 132.78, 133.09, 136.35, 137.77, 140.23, 141.0, 146.6, 146.83, 150.58. MALDI-TOF-MS: calcd for ($C_{150}H_{144}N_6O_2$): *m/z* [M^+]: 2062.1; found: *m/z* 2061.7. $C_{84}H_{72}N_4$ (EA) (%, found/calcd): C, 87.76/87.34; H, 6.73/7.04; N, 3.71/4.07.

G2-3. Compound **G0** (204 mg, 0.21 mmol), borate **8** (50 mg, 0.10 mmol). The crude product was purified by column chromatography on silica gel using chloroform/petroleum ether (2 : 1, v/v) as eluent to afford a yellow solid (197 mg, 90.0%). ^{1}H NMR (300 MHz, $CDCl_3$, 298 K) δ (ppm): 0.77 (t, $J = 7.5$ Hz, 6H, $-CH_3$), 0.87 (t, 12H, $-CH_3$), 1.08 (br, s, 12H, $-CH_2-$), 1.20–1.45 (m, 24H, $-CH_2-$), 1.88 (m, 8H, $-CH_2-$), 2.05 (br, s, 4H, $-CH_2C-$), 4.30 (t, $J = 7.2$ Hz, 8H, $-NCH_2-$), 7.14 (m, 16H, ArH and C=CH), 7.23 (m, 4H, ArH), 7.36–7.51 (m, 24H, ArH), 7.60–7.71 (m, 16H, ArH), 7.77 (d, $J = 7.2$ Hz, 2H, ArH), 8.09 (d, $J = 8.1$ Hz, 4H, ArH), 8.30 (s, 4H, ArH). ^{13}C NMR (75 MHz, $CDCl_3$, 298 K) δ (ppm): 12.99, 21.53, 25.94, 27.92, 28.69, 30.54, 42.20, 54.2, 86.44, 89.53, 97.35, 107.70, 107.89, 112.32, 117.17, 118.25, 119.02, 119.51, 120.21, 121.45, 121.82, 122.77, 122.89, 123.82, 125.03, 125.82, 126.36, 126.58, 128.18, 131.53, 135.40, 138.5, 139.00, 139.77, 145.58, 150.73. MALDI-TOF-MS: calcd for ($C_{157}H_{148}N_6$): *m/z* [M^+]: 2118.2; found: *m/z* 2118.4. $C_{157}H_{148}N_6$ (EA) (%, found/calcd): C, 88.65/88.99; H, 6.73/7.04; N, 3.56/3.97.

Fabrication and characterization of OLEDs

In a general procedure, indium-tin oxide (ITO)-coated glass substrates were etched, patterned, and washed with detergent, deionized water, acetone, and ethanol sequentially. Two types of double-layer devices were fabricated using dendrimers as hole-transporting or emitting materials: (I) ITO/**G1** or **G2-1**/Alq3/Ca: Ag; (II) ITO/**G1** or **G2**/TPBI/LiF/Al; where 8-hydroxyquinoline aluminium (Alq3) was used as an emitting/electron-transporting layer, and 2,2′,2″-(1,3,5-benzenetriyl)tris-[1-phenyl-1*H*-benimidazole] (TPBI) was used as a hole-blocking/electron-transporting layer, respectively. The active layer of dendrimer was spin-coated from chloroform solution, and the Alq3 or TPBI layer was deposited by means of conventional vacuum deposition onto the ITO-coated glass substrates at a pressure of 5×10^{-5} Pa. For devices I, the weight ration of a cathode–Ca/Ag layer is 10 : 1. The active area of the device was 4 or 5 mm^2. A quartz crystal oscillator placed near the substrate was used to monitor the thickness of each layer, which was calibrated *ex situ* using an Ambios Technology XP-2 surface profilometer. EL spectra and chromaticity coordinates were measured with a SpectraScan PR650 photometer. Current density–voltage–luminance (*J–V–L*) measurements were made simultaneously using a Keithley 4200 semiconductor parameter analyzer and a Newport multi-function 2835-C optical meter, and luminance was measured in the forward direction. All device characterizations were carried out under ambient laboratory air at room temperature.

Photoresist patterning

In a general procedure, a solution of **G2-1** with a concentration of ~1.5 wt% (5 mg of **G2-1** in 0.3 mL of 1,2-dichloroethane) was passed through a 0.5 μm PTFE filter and spin-coated onto a silica wafer at 2000 rpm for 60 s. After being dried in a vacuum oven overnight, the film was exposed to UV light with an incident intensity of ~32 mW cm^{-2} through a copper-negative mask for 15 min. The unexposed part of the film was

washed away by developing it in 1,2-dichloroethane for 60 s. After the film was dried in a vacuum oven, the photoresist pattern was photographed with an Olympus BX60 optical microscope. The fluorescence image was taken with an Olympus BX41 fluorescence optical microscope using a broad UV light source of 330–380 nm.

Acknowledgements

We are grateful to the National Science Foundation of China (no. 21034006), and the program of NCET for financial support.

Notes and references

1 C. W. Tang and S. A. Vanslyke, *Appl. Phys. Lett.*, 1987, **51**, 913.
2 J. H. Burroughes, D. D. C. Bradley, A. R. Brown, R. N. Marks, K. Mackay, R. H. Friend, P. L. Burn and A. B. Holmes, *Nature*, 1990, **347**, 539.
3 F. Hide, M. A. Diaz-Garcia, B. J. Schartz and A. J. Heeger, *Acc. Chem. Res.*, 1997, **30**, 430.
4 R. H. Friend, R. W. Gymer, A. B. Holmes, J. H. Burroughes, R. N. Marks, C. Taliani, D. D. C. Bradley, D. A. Dos Santos, J. L. Bredas, M. Löglund and W. R. Salaneck, *Nature*, 1999, **397**, 121.
5 C. D. Müller, A. Falcou, N. Reckefuss, M. Rojahn, V. Wiederhirn, P. Rudati, H. Frohne, O. Nuyken, H. Becker and K. Meerholz, *Nature*, 2003, **421**, 829.
6 S. R. Forrest, *Nature*, 2004, **428**, 911.
7 Y. Sun, N. C. Giebink, H. Kanno, B. Ma, M. E. Thompson and S. R. Forrest, *Nature*, 2006, **440**, 908.
8 J. Li and D. Liu, *J. Mater. Chem.*, 2009, **19**, 7584.
9 P. L. Burn, S.-C. Lo and I. D. W. Samuel, *Adv. Mater.*, 2007, **19**, 1675.
10 S.-C. Lo and P. L. Burn, *Chem. Rev.*, 2007, **107**, 1097.
11 S.-K. Hwang, C. N. Moorefield and G. R. Newkome, *Chem. Soc. Rev.*, 2008, **37**, 2543.
12 S.-C. Lo, R. E. Harding, E. Brightman, P. L. Burn and I. D. W. Samuel, *J. Mater. Chem.*, 2009, **19**, 3213.
13 Y. Shirota, *J. Mater. Chem.*, 2000, **10**, 1.
14 Y. Shirota, *J. Mater. Chem.*, 2005, **15**, 75.
15 Y. Shirota and H. Kageyama, *Chem. Rev.*, 2007, **107**, 953.
16 Y. Zhang, T. Wada and H. Sasabe, *J. Mater. Chem.*, 1998, **8**, 809.
17 M. Sonntag, K. Kreger, D. Hanft and P. Strohriegl, *Chem. Mater.*, 2005, **17**, 3031.
18 Z. Zhao, X. Xu, H. Wang, P. Lu, G. Yu and Y. Liu, *J. Org. Chem.*, 2007, **73**, 594.
19 H. Tanaka, S. Tokito, Y. Taga and A. Okada, *Chem. Commun.*, 1996, 2175.
20 J. Kido, K. Hongawa, K. Okuyama and K. Nagai, *Appl. Phys. Lett.*, 1994, **64**, 15.
21 C.-W. Ko, Y.-T. Tao, J. T. Lin and K. R. J. Thomas, *Chem. Mater.*, 2002, **14**, 357.
22 K. Brunner, A. Dijken, H. nBörner, J. J. A. M. nBastiaansen, K. M. M. Kiggen and B. M. W. Langeveld, *J. Am. Chem. Soc.*, 2004, **126**, 6035.
23 Y.-C. Chen, G.-S. Huang, C.-C. Hsiao and S.-A. Chen, *J. Am. Chem. Soc.*, 2006, **128**, 5592.
24 Z. Jiang, X. Xu, Z. Zhang, C. Yang, Z. Liu, Y. Tao, J. Qin and D. Ma, *J. Mater. Chem.*, 2009, **19**, 7661.
25 Y. Tao, Q. Wang, C. Yang, C. Zhong, K. Zhang, J. Qin and D. Ma, *Adv. Funct. Mater.*, 2010, **20**, 304.
26 Z. Jiang, Y. Chen, C. Yang, Y. Cao, Y. Tao, J. Qin and D. Ma, *Org. Lett.*, 2009, **11**, 1503.
27 N. Tamoto, C. Adachi and K. Nagai, *Chem. Mater.*, 1997, **9**, 1077.
28 K. Itano, H. Ogawa and Y. Shirota, *Appl. Phys. Lett.*, 1998, **72**, 636.
29 Q.-X. Tong, S.-L. Lai, M.-Y. Chan, K.-H. Lai, J.-X. Tang, H.-L. Kwong, C.-S. Lee and S.-T. Lee, *Chem. Mater.*, 2007, **19**, 5851.
30 K. R. J. Thomas, J. T. Lin, Y.-T. Tao and H.-W. Ko, *Chem. Mater.*, 2002, **14**, 1354.
31 X.-Y. Cao, X.-H. Liu, X.-H. Zhou, Y. Zhang, Y. Jiang, Y. Cao, Y.-X. Cui and J. Pei, *J. Org. Chem.*, 2004, **69**, 6050.
32 A. Kimoto, J.-S. Cho, M. Higuchi and K. Yamamoto, *Macromolecules*, 2004, **37**, 5531.
33 Y. Jiang, L. Wang, Y. Zhou, Y.-X. Cui, J. Wang, Y. Cao and J. Pei, *Chem.–Asian J.*, 2009, **4**, 548.
34 H. Xia, J. He, B. Xu, S. Wen, Y. Li and W. Tian, *Tetrahedron*, 2008, **64**, 5736.
35 Z. Zhao, J.-H. Li, X. Chen, X. Wang, P. Lu and Y. Yang, *J. Org. Chem.*, 2009, **74**, 383.
36 J.-M. Kim, T.-E. Chang, J.-H. Kang, K. H. Park, D.-K. Han and K.-D. Ahn, *Angew. Chem., Int. Ed.*, 2000, **39**, 1780.
37 J. Liu, J. W. Y. Lam and B. Z. Tang, *Chem. Rev.*, 2009, **109**, 5799.
38 G. Koeckelberghs, M. Vangheluwe, I. Picard, L. D. Groof, T. Verbiest, A. Persoons and C. Samyn, *Macromolecules*, 2004, **37**, 8530.
39 Z. Zhou, F. Li, T. Yi and C. Huang, *Tetrahedron Lett.*, 2007, **48**, 6633.
40 R. Grisorio, C. Piliego, P. Fini, P. Cosma, P. Mastrorilli, G. Gigli, G. P. Suranna and C. F. Nobile, *J. Phys. Chem. C*, 2008, **112**, 7005.
41 Z. Li, Z. Li, D. Di, Z. Zhu, Q. Li, Q. Zeng, K. Zhang, Y. Liu, C. Ye and J. Qin, *Macromolecules*, 2006, **39**, 6951.
42 Z. Li, Y. Liu, G. Yu, Y. Wen, Y. Guo, L. Ji, J. Qin and Z. Li, *Adv. Funct. Mater.*, 2009, **19**, 2677.
43 P.-H. Aubert, M. Knipper, L. Groenendaal, L. Lutsen, J. Manca and D. Vanderzande, *Macromolecules*, 2004, **37**, 4087.